

# Generation and propagation of solitary wave over a steep sloping beach

Zouhaier Hafsia <sup>(1)</sup>, Mehdi Ben Haj <sup>(2)</sup>, Hedi Lamoumi <sup>(3)</sup>, Khelifa Maalel <sup>(4)</sup> and Ridha Zgolli <sup>(5)</sup>

<sup>(1-5)</sup> ENIT. Laboratoire d'Hydraulique B.P. 37. Le Belvédère, 1002 Tunis, Tunisia

E-mail : [Zouhaier.Hafsia@enit.rnu.tn](mailto:Zouhaier.Hafsia@enit.rnu.tn)

## **Abstract**

A numerical model has been developed to solve the unsteady Navier–Stokes equations together with a convective equation describing the flow surface profile and with the appropriate boundary conditions. In order to generate nonlinear solitary wave on constant depth, an appropriate mass source term is added for the equation of mass conservation in the internal flow region. This model is implemented in the industrial Computational Fluid Dynamics code : PHOENICS (Parabolic Hyperbolic Or Elliptic Numerical Integration Code Series). The numerical wave generation is validated by comparisons of numerical results with the analytical solutions and show that the solitary wave is very accurately generated. The propagation of the solitary wave in constant water depth indicated that the wave preserved its permanent form and the same wave velocity.

This model is then used to simulate the nonbreaking runup and rundown caused by the solitary wave passing over impermeable steep plane beach. The numerical results are compared with experimental data of Lin and al. (1999) and show that the free surface profiles and vertical velocity component are accurately predicted during the runup and rundown process. However, the comparisons of horizontal velocity component show small discrepancy during the rundown process and larger discrepancies during the runup process.

## **1- Introduction**

The design and the protection of beaches and harbors require testing of these coastal structures for different wave conditions. To study wave and structure interaction near shoreline region, solitary waves are used which approximately model steep waves on beaches. In coastal engineering, the solitary wave is also used to represent long free-surface waves such as wave generated by wind (wind waves) or earthquakes (tsunamis). In the early research, physical model is commonly used to study ocean wave propagation, shoaling, breaking or runup over a slope.

Over the past fifty years, the wave structure interaction has been the object of numerous theoretical studies. Using a nonlinear transformation of shallow water wave equation, Synolakis (1987) obtained analytical solution for the maximum runup height for non breaking solitary waves propagating over constant depth and determined breaking criterion during runup and rundown processes.

More recently, numerical wave flumes (2D) have been developed to reproduce wave generation and propagation. Grilli (1994), used a nonlinear potential flows based on Boundary integral formulations to study wave profiles during breaking of solitary wave on plane beach with gradual and steep inclined plane.

The Boussinesq equations have been widely employed to study runup and rundown along sloping beach. The standard form of these equations can be derived from Euler equations ignoring rotational and dissipation effects (Kim, 2006). This model include the first order effects of non linearity and dispersion and are valid for weakly nonlinear and dispersive waves. This approach is useful for large-scale computations. Zelt (1991) used a Lagrangian form of this model to reproduce the shoreline movement induced by solitary propagating

wave. The Boussinesq equations has been extended to include higher order effects of non-linearity and dispersion and nonlinear of this formulation in order to study wave shoaling and runup (Lynett and al. 2002). Using energy velocity instead of phase velocity, Kim (2006), show that the source function in the horizontally two-dimensional wave models based on Boussinesq equations is identical to the source function in the three-dimensional continuity equation. Maiti (1999) studied interaction of solitary waves with impermeable inclined walls and evaluate pressures and forces during the reflection by prescribing the motion of the piston wave maker. In later study, the boundary conditions at upstream are functioned as a wavemaker to generate the desired conditions

However, this model is not capable to represent accurately highly nonlinear wave breaking processes, air entertainment and turbulence. Models taking into account the vertical variation of the flow can better reproduce the breaking waves where wave becomes very asymmetric. To take into account energy dissipation over the entire range of water depth, the complete Navier-Sotkes (N-S) is used for non breaking solitary wave on steep plane beach and Reynolds-averaged Navier-Stokes (RANS) for breaking wave on gradual plane beach, Lin and al. (1999). The breaking of cnoidal wave in a sloping plane beach is investigated by Lin and Liu (1998) by developing numerical model for predicting turbulence characteristics for shoaling. In the later study, the wave is generated directly without using the wavemaker theory by prescribing the water surface elevation and mean velocity components in both horizontal and vertical directions on the upstream boundary. The pressure is unknown but can be computed from continuity equation. Based on (RANS), Park and al. (2003) developed a 3D model for investigate nonlinear wave interaction with arctic structure and show that the flow viscosity affects free surface profiles.

In this paper, we are interested on generation and propagation of solitary wave over uniform slope by Navier-Stokes solver with the Volume of Fluid Fraction (VOF) method which is capable to model fully overturning waves even with fluid re-attachment. The PHOENICS code is used to implement the additional source terms relative to the equation of mass conservation and the momentum equation in the vertical direction. With this code, more complicated problems such as the addition of turbulence in breaking wave and three-dimensional flow induced by wave structure interaction can be investigated.

## 2- Governing equations

### 2-1 Physical problem description

In this study, we consider the propagation, in the vertical plane, of the solitary wave in undisturbed water depth,  $d = 0.16$  m, and passing over a plane beach of slope angle  $\beta = 30^\circ$  (figure 1).

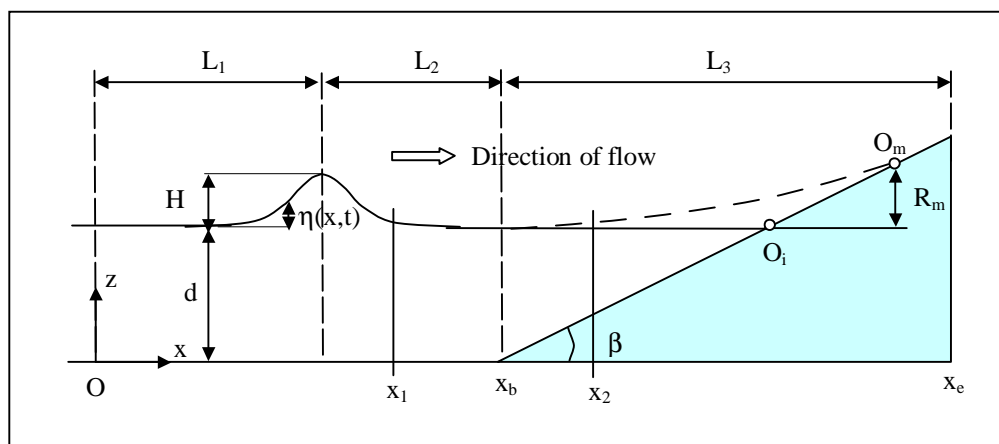


**Figure 1 : Schematic diagram of solitary wave propagating over inclined plane**

The toe of the beach is located at  $x_h = 8.12$  m from the  $x$  origin. The offshore incident solitary wave height is  $H = 0.027$  m (the ratio of wave height to water depth ratio is  $\frac{H}{d} = 0.17$ ). The initial shoreline is located at  $Q_i$  and after maximum runup, the shoreline is located at  $Q_m$ . At this point, the wave have has a maximum runup denoted by  $R_m$ . Lin and al. (1999) conducted a set of experiments over this geometric configuration in a wave flume that has a dimension of 30 m long, 0.6 m wide and 0.9 m deep. The free surface profiles are obtained by the PIV (Particle Image Velocimetry) system and the velocity components are obtained by determination of the seeding particle displacements. Two measurement section located at  $x_1 = 8.03$  m and  $x_2 = 8.17$  m are used to validate the simulated velocity components profiles.

## **2-2 Transport Equations**

To generate numerically a given wave in two-dimensional flow, a mass source function is required for the mass conservation equation and a friction source for dumping wave at open boundary is added in the vertical momentum equation. Assuming incompressible fluid, the modified mass conservation equation is written as :

$$\frac{\partial u}{\partial x} + \frac{\partial w}{\partial z} = s(t) \quad (1)$$

Where,  $u$  and  $w$  are the velocity components respectively in  $x$  and  $z$  directions.  $s(t)$  is an added mass source term depending on the type wave to be generated.

For solitary wave, assuming that the wave is generated at  $x = 0$ , the local free surface elevation function of the time  $t$  is given by the following equation:

$$h(t) = H \operatorname{sech}^2[k(x_s - Ct)] \quad (2)$$

With  $\operatorname{sech}()$  is the hyperbolic secant;  $H$  : wave height;  $C$  the wave celerity given by :

$$C = \sqrt{gd} \quad (3)$$

The parameter  $k$  is given by :

$$k = \sqrt{\frac{3H}{4d^3}} \quad (4)$$

The length of a solitary wave is theoretically infinitely long. However for practical purposes we can define an arbitrarily wavelength as :

$$l = \frac{2p}{k} \quad (5)$$

The apparent wave period is defined as :

$$T = \frac{l}{C} \quad (6)$$

The distance  $x_s$  is introduced to make the source function is negligible at initial time :

$$x_s = \frac{4d}{\sqrt{H/d}} \quad (7)$$

This implies that 99 % of solitary mass can be generated by the source function at  $t = 0$ . According to Lin and Liu (1999), the corresponding mass source term is given by :

$$s(t) = \frac{2 C h(t)}{A} \quad (8)$$

In laminar viscous flow, the dynamic transport equation describing the velocity component in the horizontal direction is:

$$\frac{\partial u}{\partial t} + u \frac{\partial u}{\partial x} + w \frac{\partial u}{\partial z} = -\frac{1}{r} \frac{\partial P}{\partial x} + \nu \left( \frac{\partial^2 u}{\partial x^2} + \frac{\partial^2 u}{\partial z^2} \right) \quad (9)$$

A dissipation zone is used for damping the wave amplitude at the outlet boundary. In this region, a friction source term is added to the vertical velocity component within the momentum transport equation in the vertical direction:

$$\frac{\partial w}{\partial t} + u \frac{\partial w}{\partial x} + w \frac{\partial w}{\partial z} = -g - \frac{1}{r} \frac{\partial P}{\partial z} + \nu \left( \frac{\partial^2 w}{\partial x^2} + \frac{\partial^2 w}{\partial z^2} \right) - g \gamma \quad (10)$$

With : P the pressure;  $\nu$  : kinematic viscosity;  $\rho$  : fluid density; g : gravitational acceleration.  $\gamma$  : is a dumped function equals to zero except for the added dissipation zone.

$$g(x) = a x + b \quad (9)$$

Where,  $x_s < x < x_e$  (subscripts s, e mean starting and end point of damping zone).

$\alpha$  : is the control parameter

The dumping force in horizontal direction is not considered (in Equation 9) in order to avoid the velocity dumping in the uniform horizontal flow.

The mass source term introduce the following source term in the VOF transport equation,

$$\frac{\partial F}{\partial t} + \frac{\partial}{\partial x}(F u) + \frac{\partial}{\partial z}(F w) = F s \quad (11)$$

A cell with an  $F = 0$  refers to an empty cell, the one with  $0 < F < 1$  is a surface cell and a cell with  $F = 1$  is a water full cell, [Hirt and al. \(1981\)](#).

The wave propagation is considered as a two phases flow involving water phase and air phase. We assume that the sliding between the two phases is negligible and that there is no mass exchange across the interface. Hence, the velocity field at the free surface is continued.

### **2-3 Initial and boundary conditions**

To solve the governing equations of the N-S model, four boundary conditions are needed : free surface, bottom, upstream and downstream boundaries.

The free-surface boundary conditions consist of kinematic and dynamic boundary conditions. The kinematic free surface boundary condition states that the fluid particles of the free surface always stay on the free surface at any time and is written as :

$$\frac{\partial h}{\partial t} + u \frac{\partial h}{\partial x} = w \quad \text{at } z = d + h(x, t) \quad (12)$$

where  $\eta(x,t)$  is the water surface elevation.

The dynamic free surface boundary conditions requires that, along the free surface boundary, the normal stress is equal to the atmospheric pressure and the tangential stress is zero.

The no-slip boundary condition is imposed on the solid boundaries (the bottom and the inclined plane of the beach).

At the open boundary condition, a dissipation zone is added in order to avoid wave reflection at this region. Within such zone, located at the left of the computation domain, it is

advantageous to consider in addition to the dumping friction force, a numerical dissipation by applying a coarse grids in the dissipation zones. The Neumann boundary condition is specified at the upstream and downstream boundaries.

The initial condition considered is a still water with no wave or current motion.

## **2-4 Numerical scheme in the PHOENICS code**

In the PHOENICS code, the governing equations are discretized using a finite volume method applied to a staggered Cartesian grid system (Patankar, 1980). All the velocity components are defined at the midpoints of the cell faces; whereas, the scalar flow variables (pressure and water surface elevation) are defined at the center of the cells.

The implicit method is used to discrete the time derivative. The convection terms are discretized by hybrid scheme. To satisfy the continuity equation, pressures are iteratively adjusted in each cell until that the discrete divergence in the continuity equation is zero. Then, the velocity changes caused by each pressure correction are added to the temporary velocity field. The Van Leer scheme with Total Variation Diminishing (TDV) approach is adopted in order to overcome the discontinuities of flow variables at the interface.

## **3- Numerical results and discussion**

### **3-1 Solitary wave generation in constant depth**

Preliminary numerical tests are made to test the generation method with addition of internal mass source functions to the mass conservation. The total horizontal length of computational domain is 8.62 m including 6 m for the dissipation zone. The numerical computation is conducted with  $NX = 161$  and  $NZ = 101$  grids respectively in  $x$  and  $z$  directions. The finest grid size in horizontal and vertical directions are chosen as  $\Delta x = 0.0125$  m and  $\Delta z = 0.0018$  m, respectively. The time increment is  $\Delta t = 0.0067$  s.

Due to the differences between the lengths in constant depth region used in numerical and experimental cases and the generation mechanism used, results are synchronized at the time where the incident wave crest crossed the location  $x = 7.45$  m in the computation domain (for  $t = 2.27$  s). For this time origin, no adjustment is made to the experimental propagation time given by Lin and al. (1999).

The numerical results for free-surface elevations at this time are shown in Fig. 2. It is noted that the numerical results differ slightly from the PIV data. At this time, the shape of the solitary wave profile is not affected by the sloping beach and is similar with the theoretical solitary wave solution.

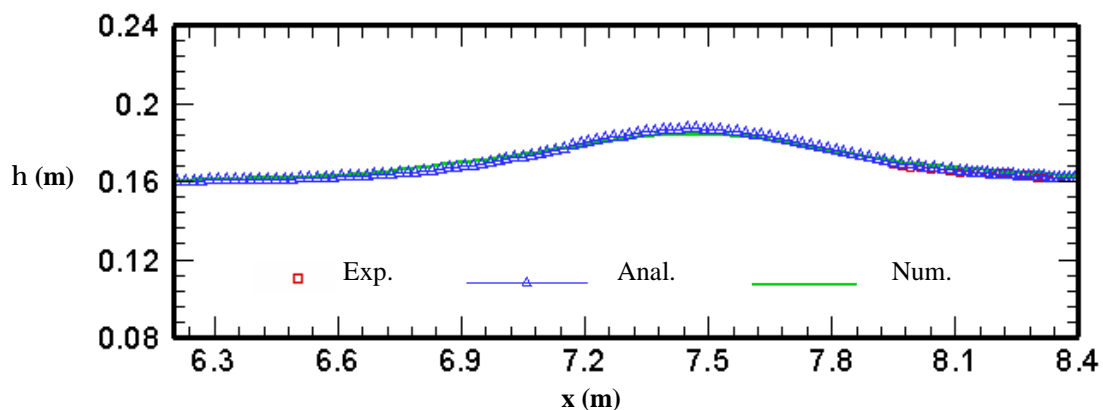
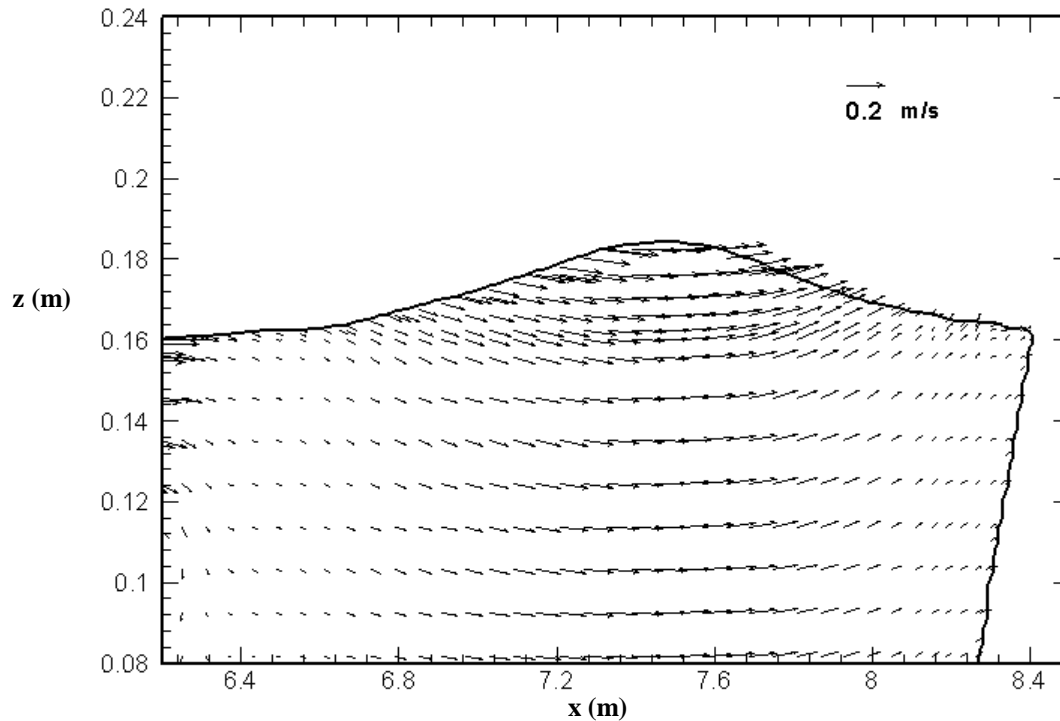


Figure 2 : Comparison of the experimental, analytical and numerical solitary wave profiles at  $t = 2.27$  s.

The velocity field induced by the solitary wave is shown in figure 3 and indicated that the wave is propagating from left to right.



**Figure 3 : Numerical free surface profile and velocity distribution induced by solitary wave at  $t = 2.27$  s.**

The velocity below the wave crest is greater than in the region where the free surface is equal to the undisturbed water level. This proves that solitary wave is very well generated by the proposed N-S model. Using mass source function method for the generation of solitary wave, numerical tests show that the reflected wave will not interfere with the wave generation process. This implies that this generation method can be used for long duration simulation of coastal wave dynamics when reflected waves are present.

### **3-2 Interaction of solitary wave and steep beach**

From the experimental results of Lin and al. 1999, the interaction between solitary wave and a steep beach is characterized by three phases : the first runup, the rundown and the second runup. To analyze the runup and rundown mechanism we have reported in figs 4 (a to f) the simulated free surface profiles together with the computed velocity field at different stage of the runup and rundown processes.

Fig 4-a) shows the velocity field at  $t = 2.97$  s. In the start of the first runup process, the fluid particles climb up parallel to the slope. The velocity is maximum at the shoreline and decreased away from the shoreline. At this time, the comparison of the N-S numerical free surface profiles and the experimental results show that the numerical results overestimate the free surface profile near the shoreline zone.

At the instance when the wave almost reaches its highest runup point  $R_m$  ( $t = 3.17$  s), the numerical results indicates that  $R_m = 0.071$  m : 2.63 greater than the wave height  $H$  (fig. 4-b). At this time, the major fluid particles are reflected against the sloping beach except very small region in the vicinity of the shoreline where the particles still moves upward. The comparison between numerical and experimental measurements indicates that the free surface elevation are accurately predicted.

At  $t = 3.37$  s, the wave is running down on the slope (fig 4-c), and at  $t = 3.77$  s the wave is approaching its maximum rundown point (Fig 4-d). After the wave reaches its maximum rundown point, the secondary runup occurred. The secondary runup process is shown in fig 4-e ( $t = 3.97$  s) and fig 4-f ( $t = 4.17$  s). The secondary maximum runup point is much smaller than the first one. In fact, at this time the quasi totality of the wave has been reflected by the steep slope.

In order to analyze the three phases induced by the interaction of solitary wave and inclined plane, we reported in figs 5 to 8 the vertical distribution of the velocity components at the measurements section  $x_1$  (in the constant water depth region) and  $x_2$  (on inclined plane of the beach). The numerical velocity profiles are compared to the experimental data of Lin and al. (1999).

At section  $x_1$ , and during the runup process, the horizontal velocity component  $u$  is nearly uniform with positive values (fig 5). At the maximum runup,  $u$  is negative due to running down motion of fluid particles in constant water depth and on the beach. However, at section  $x_2$ , the vertical distribution of  $u$  is non uniform; it increase linearly from the inclined plane to the free surface (fig 6). The comparison of numerical and experimental results show that, the horizontal velocities  $u$  are underestimated during the runup process. The non uniform vertical distribution of  $u$  on the beach indicates that the shallow water equations assuming the long wave approximation can not be used to predict accurately the runup process.

At section  $x_1$ , and during the runup process, the vertical velocity component  $w$  is negligible (fig 7). During the rundown process, strong vertical variations of  $w$  component is observed. At section  $x_2$  (fig 8) and at the start of the secondary runup ( $t = 3.97$  s), the vertical motion is so strong that the magnitude of vertical velocity component  $w$  near free surface is much larger than the horizontal velocity component  $u$  (fig.6 and 8). The comparison of experimental and numerical vertical velocity profiles is better during the rundown process at section  $x_1$  and  $x_2$ .

Numerical tests are conducted assuming that the energy dissipation due to viscous is considered as negligible. Hence, by neglecting the diffusion terms in the momentum equation the N-S equations are reduced to Euler's equations for inviscid fluids. Numerical results show that, for non breaking wave runup, viscous effect is not important.

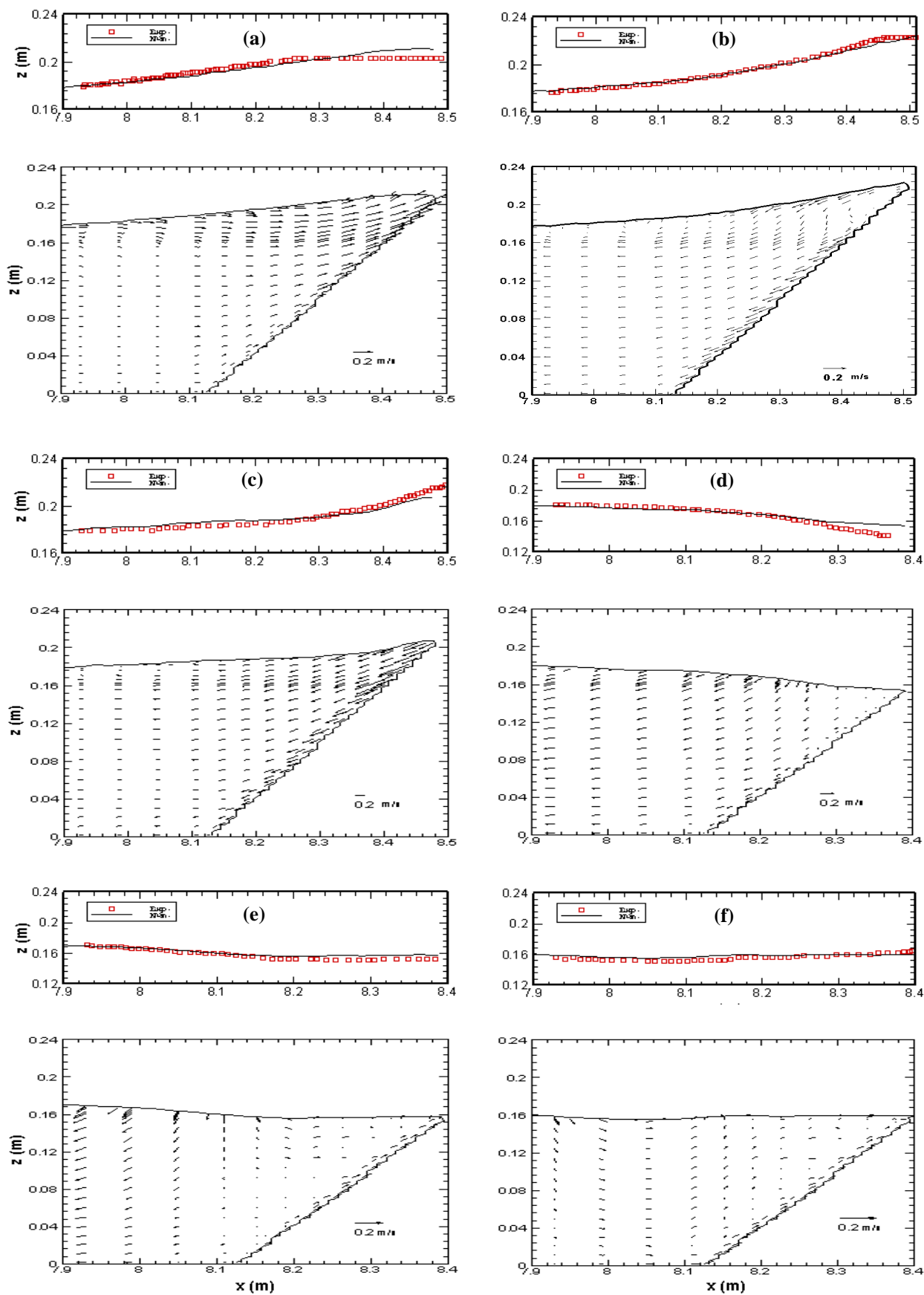


**Figure 4 : Numerical and experimental free surface profile and computed velocity field in the vicinity of the beach at different time : a)  $t = 2,97$  s; b)  $t = 3,17$ ; c)  $t = 3,37$ ; d)  $t = 3,77$ ; e)  $t = 3,97$  f)  $t = 4,17$  .**



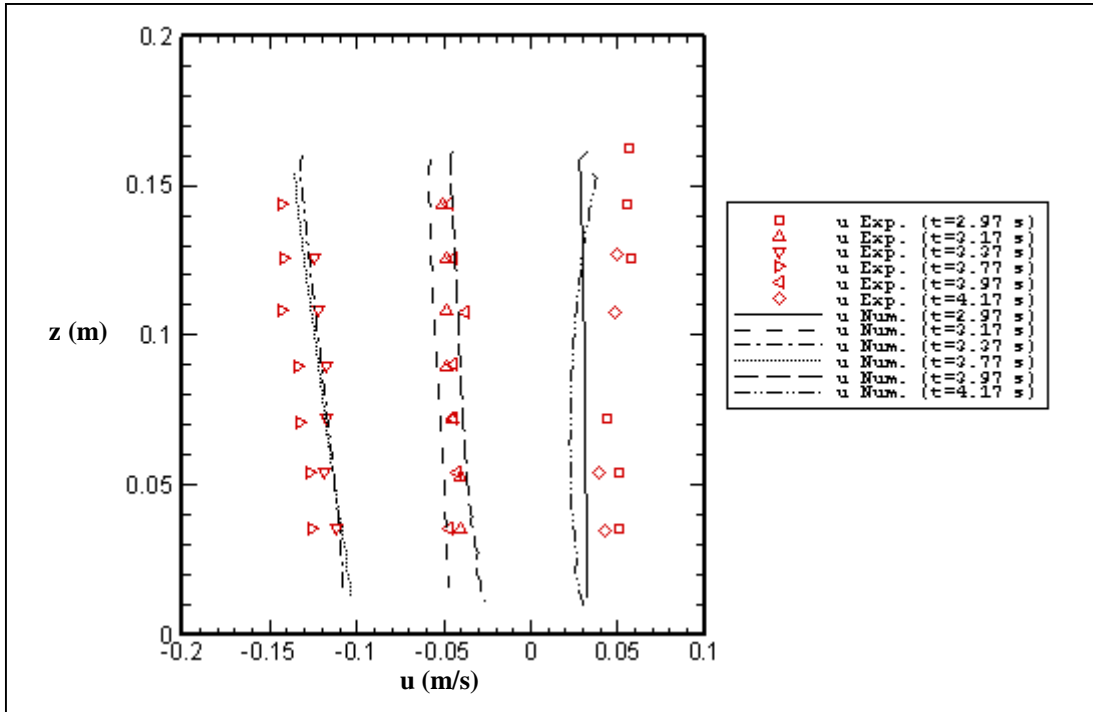


Figure 5 : The comparison of horizontal velocity between the experimental measurements and the numerical results at section  $x_1$  for different times.

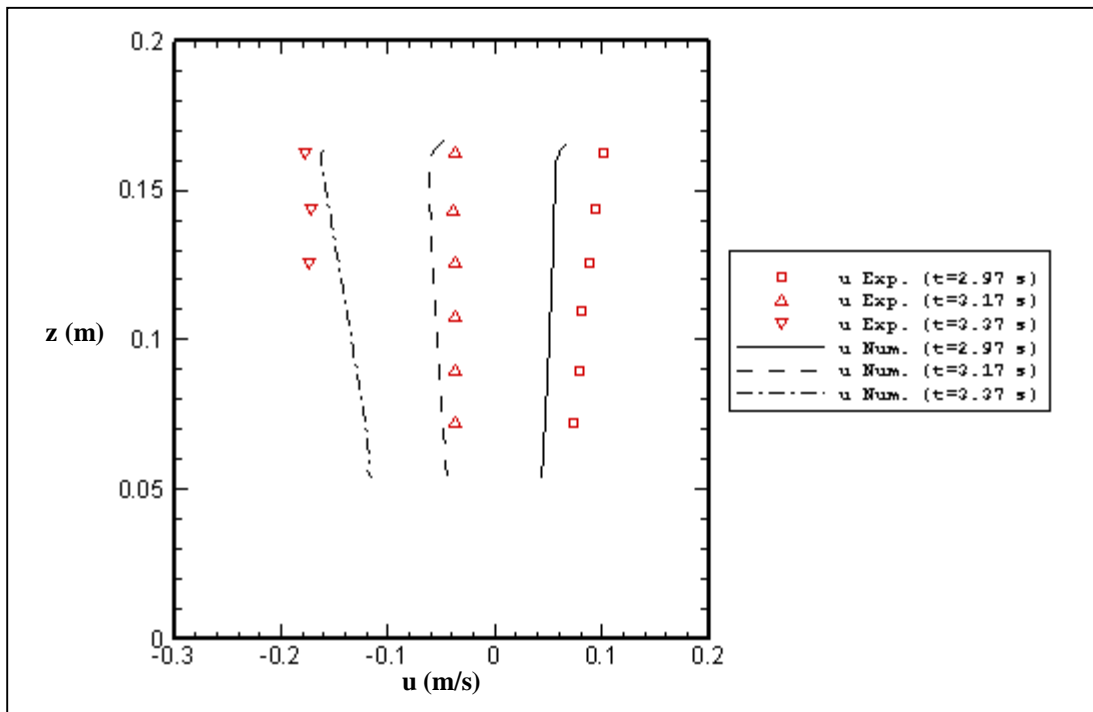


Figure 6 : The comparison of horizontal velocity between the experimental measurements and the numerical results at section  $x_2$  for different times.

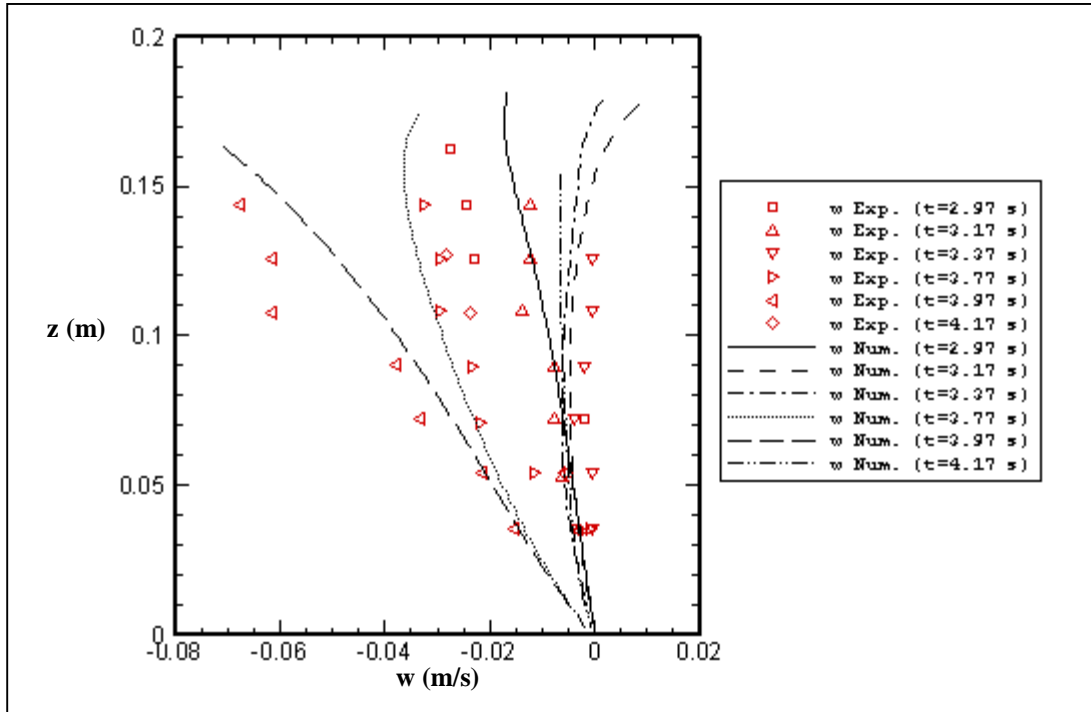


Figure 7 : The comparison of vertical velocity between the experimental measurements and the numerical results at section  $x_1$  for different times.

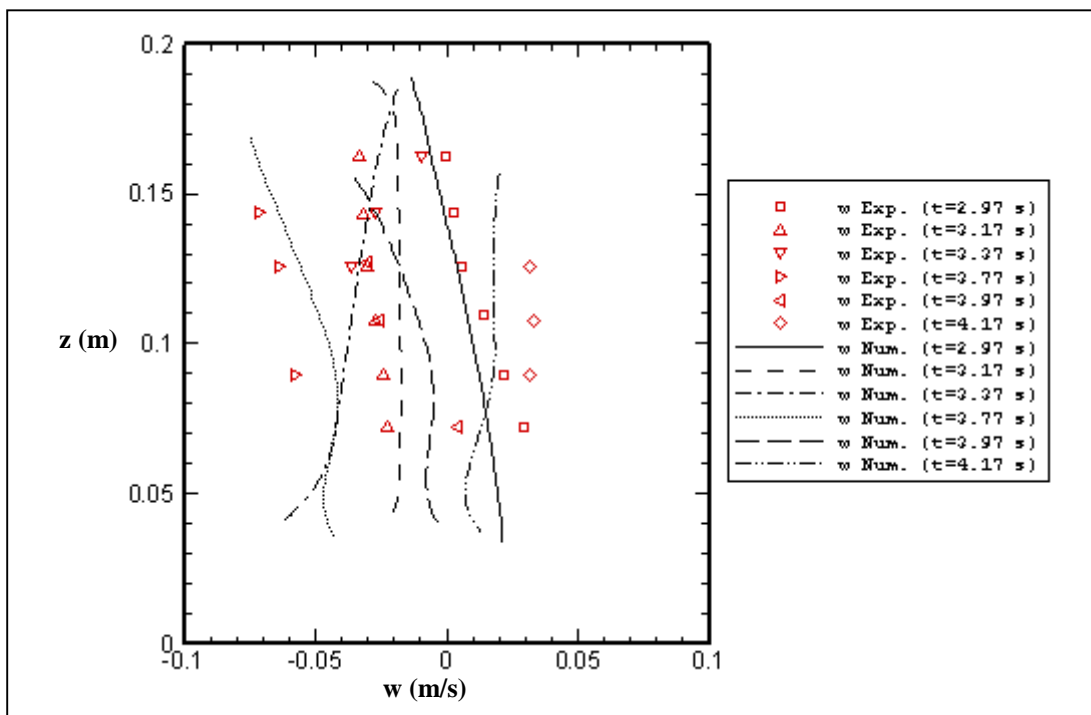


Figure 8 : The comparison of vertical velocity between the experimental measurements and the numerical results at section  $x_2$  for different times.

## **4- Conclusion**

Based on the Navier–Stokes solver of the PHOENICS code, the generation and propagation of solitary wave over impermeable steep beach are computed and analyzed. Adding internal mass source function to the mass conservation equation generates the solitary wave and a friction force is added to the vertical momentum equation to avoid reflection at open boundary. The comparison of the generated solitary wave and theoretical wave show that this generation method predicts very accurately the wave celerity and its permanent shape.

In order to validate the developed model, the nonbreaking runup and rundown processes along a steep beach is considered. The comparison between experimental measurements and numerical computations of free surface profiles and vertical velocity component demonstrate the overall agreement of these flow variables. The vertical velocities are accurately predicted, however, some disagreements are observed for horizontal velocity component during the runup process. In future study we propose to analyze the effect of turbulence on the breaking wave along a gradual beach.

## **Acknowledgments**

The writers are grateful to Professor Pengzhi Lin for providing original figures of experimental data.

## **References**

- Grilli S. T.; Subramanya R. ; Svendsen I. A. ; Veeramony J. - Shoaling of solitary waves on plane beaches. *Journal of Waterway, Port, Coastal, and Ocean Engineering*. Vol. 120 N° 6 (1994).
- Hirt, C.W. and Nichols, B.D. -. Volume of fluid (VOF) method for the dynamics of free boundaries. *J. Comp. Phys.* 39, pp. 201–225 (1981).
- Kim Gunwoo - Internal generation and transformation of waves over rapidly varying topography. PhD School of Civil, Urban & Geosystem Engineering. Seoul National University (2006).
- Lin Pengzhi, Chang Kuang-An, and Liu Philip L.-F. - Runup and rundown of solitary waves on sloping beaches. *Journal of Waterway, Port, Coastal, and Ocean Engineering*. Vol. 125 N° 5 (1999).
- Lin Pengzhi, Liu Philip L-F - A numerical study of breaking waves in the surf zone. *Journal of Fluid Mechanics*. Vol 359, 239-264 (1998).
- Lin P. and Liu P. - Internal wave-maker for Navier-Stokes equations models. *Journal of waterway, port, coastal, and ocean engineering*. Vol 125 N° 4, 207-215. July-august (1999).
- Lynett Patrick J., Wu Tso-Ren, Liu Philip L.-F. - Modeling wave runup with depth-integrated equations. *Coastal Engineering* 46 (2002) 89–107
- Maiti Sangita, Sen Debabrata - Computation of solitary waves during propagation and runup on a slope. *Ocean Engineering* 26 (1999) 1063–1083
- Park J.-C., Kim M.-H., Miyata H., Chun H.-H. - Fully nonlinear numerical wave tank (NWT) simulations and wave run-up prediction around 3-D structures. *Ocean Engineering* 30 (2003) 1969–1996.
- Patankar S.V. - *Numerical Heat Transfer and Fluid Flow*. McGraw (1980).
- Synolakis C. E. (1987) The runup of solitary waves. *J. Fluid Mech.* Vol 185. pp 523–545

Zelt J.A. - The run-up of nonbreaking and breaking solitary waves. Coastal Engineering, 15 (1991) 205-246.